Statistical Analysis and Probabilistic Verification of Stress-induced Signaling Pathways

Yinjiao Ma

Department of Biostatistics, College for Public Health & Social Justice, Saint Louis University, St. Louis, MO, USA

Lu Feng

Department of Mathematics and Computer Science, Saint Louis University, St. Louis, MO 63103, USA

Yusong Guo

Division of Life Science, Hong Kong University of Science and Technology, Clear Water Bay, Kowloon, Hong Kong

Haijun Gong

Department of Mathematics and Computer Science, Saint Louis University, St. Louis, MO 63103, USA
Corresponding Author, E-mail: hgong2@slu.edu

Abstract:

Recent studies reveal that the mysregulation of endoplasmic reticulum (ER) stress signaling pathways is implicated in the pathogenesis of several diseases. ER is a major hub for the protein synthesis, modification and sorting, and it also regulates several signaling pathways in the cell cycle progression. Disturbance of endoplasmic reticulum could induce an unfolded protein response, which is a self-protective mechanism. Graphical lasso method was first used to infer the undirected subnetworks of ER stress signaling from microarray data. Then, we construct a stochastic model to describe the crosstalk of three major signaling pathways induced by the ER stress, and apply a probabilistic model checking technique to formally analyze the temporal logic properties of the model, which is written in the PRISM language. This verification technique can both qualitatively and quantitatively verify the signaling pathway model using the sequential probability ratio test and confidence interval estimation method respectively.

Keywords: Endoplasmic reticulum; signaling pathway; cancer; Alzheimer's disease; graphical lasso; probabilistic model checking; PRISM; sequential probability ratio test; confidence interval estimation.

Biographical notes: Yinjiao Ma is currently pursuing a Master's degree in the Department of Biostatistics, College for Public Health & Social Justice at the Saint Louis University. Her research is supervised by Dr. Haijun Gong.

Lu Feng was an undergraduate student in the Department of Mathematics and Computer Science at the Saint Louis University. Her research was supervised by Dr. Haijun Gong.

Yusong Guo is an assistant professor in the Division of Life Science at Hong Kong University of Science and Technology, and he received his PhD in Cell Biology from Carnegie Mellon University. His research interests include intracellular trafficking of signaling receptors and how this influences cell signaling.

Haijun Gong is an assistant professor in the Department of Mathematics and Computer Science at the Saint Louis University. He received his PhD in Physics from Carnegie Mellon University. His research interests include the bioinformatics, computational biology, machine learning and model checking.

1 Introduction

The endoplasmic reticulum (ER) is a major communication hub for the early secretory transport pathway that regulates the protein and lipid synthesis, protein modification and sorting, and also for some signaling pathways that regulate cell cycle progression [35]. External stimuli, genetic mutations or some pathological conditions, e.g., the hypoxia and viral infection, could induce cellular stress and abnormal accumulation of unfolded proteins in the ER, leading to the activation of an unfolded protein response (UPR) [22], which is an evolutionarily conserved cellular process. UPR is a self-protective mechanism which could ameliorate the abnormal accumulation of unfolded proteins. Recent clinical and experimental studies revealed that, mysregulation of early secretory pathway and dysfunction of the ER stress signaling are implicated in the pathogenesis of cancer, Alzheimer's disease (AD), diabetes and heart disease [21, 1, 31, 30].

Prolonged or severe ER stress can activate both apoptosis (cell death) and survival signaling pathways. Somatic mutations and deregulation of key signaling pathways induced by ER stress [22, 35] might be associated with many genetic diseases. Modern microarray technique allows biologists to measure the genes' expression level and find genetic mutations from hundreds of samples in a quantitative way. Bioinformatics methods [38, 18] have been developed to identify several genetic signatures and signaling pathways that are frequently altered in the cancer. Investigation of these somatic mutations and signaling pathways will provide insights into the mechanism of ER stress, and help develop effective strategies for the early diagnosis and treatment of some diseases.

Previous studies have identified several signaling pathways initiated by the ER-resident transmembrane proteins which can sense the accumulation of unfolded proteins and regulate the cell cycle progression, including the protein kinase RNA-like ER kinase (PERK), inositol-requiring enzyme 1 (IRE1) and membrane-bound transcription factor ATF6. Some pathways regulated by the ER and Golgi apparatus can activate both survival and apoptosis signaling pathways in response to external stress. Computational biologists have proposed different statistical inference algorithms [33, 26, 36, 27, 37, 40, 16], formal verification techniques [10, 41, 19, 2, 13, 14] and simulation methods [7, 9, 8] to identify genetic signatures and analyze important signaling networks. Statistical analysis and computational modeling are helpful to study the roles of ER stress-induced signaling pathways in the cell cycle progression. Several secretory and signaling pathways, including

P53, RAS and NFκB, have been analyzed using discrete event simulation [9, 8], rule-based modeling [12, 11], Boolean and discrete value [13, 17] methods. Since the signaling pathway is complex due to a large amount of biochemical reactions, it is not efficient to apply traditional methods to analyze large networks. Our previous work had proposed and successfully applied statistical model checking [12, 11] and symbolic model checking [13, 14, 16] techniques to formally verify some signaling pathways in the cancer cell. In [14], we extend the synchronous SMV and apply an asynchronous model checking method to investigate the ER-Golgi-regulated signaling pathways. Using the SMV model checker, we can only qualitatively check some temporal logic formulas related to the cancer and Alzheimer's disease.

In this work, we first apply graphical lasso algorithm to infer undirected models of signaling subnetwork regulated by some selected genes which are important in the ER stress signaling from microarray data. Since the inference of these models is sensitive to the values of tuning parameters, we then construct a stochastic model based on previous studies to simulate the crosstalk of three signaling pathways induced by ER stress. Later, a probabilistic model checking technique is applied to formally analyze the temporal logic properties describing some biochemical reactions and molecular mechanisms in the network, which is written in the PRISM language. Compared with the symbolic model checking method, this PRISM verification technique can both qualitatively and quantatively verify the signaling pathway model using sequential probability ratio test and confidence interval estimation methods.

2 Stress-induced Subnetwork Inference

The microarray data consist of n i.i.d. (Independent and identically distributed) observations $\mathbf{X_1}, \ldots, \mathbf{X_n}$ measuring p genes, and we assume $\mathbf{X_i} \sim N(\mu, \mathbf{\Sigma})$ with a mean vector $\mu \in R^p$ and $p \times p$ covariance matrix $\mathbf{\Sigma}$. The log-likelihood function can be expressed as

$$l(\mathbf{X_1}, \ldots, \mathbf{X_n}; \mu, \Theta) \propto \frac{n}{2} \log\det\Theta - \frac{n}{2}\mathrm{tr}(\Theta\mathbf{S}),$$

where $\Theta = \Sigma^{-1}$ is the precision matrix, $\mathbf{S}$ is an observed covariance matrix of the microarray data.

The element θ_{ij} in the precision matrix describes the dependence relationship between two genes, that is, $\theta_{ij} = 0$ implies a conditional independence between two genes given the rest, while $\theta_{ij} \neq 0$ indicates a dependence. So, estimation of the precision matrix Θ will help us infer an undirected Gaussian graphical model. Friedman *et al.* [6] proposed a penalized regression method, called graphical lasso, to build undirected graphs by panalizing the off-diagonal elements of Θ with an $L1$ norm. The optimization problem is to maximize the penalized log likelihood function

$$\underset{\Theta}{\text{maximize}}\, l(\mathbf{X_1}, \ldots, \mathbf{X_n}; \mu, \Theta) = \underset{\Theta}{\text{maximize}}\{\log\det\Theta - \mathrm{tr}(\mathbf{S}\Theta) - \lambda||\Theta||_1\},$$

which is equivalent to solving the following equation

$$\frac{\partial}{\partial\Theta} l(\Theta) = \Theta^{-1} - \mathbf{S} - \lambda \cdot sign(\Theta) = 0,$$

where $||\Theta||_1 = \sum_{ij} |\theta_{ij}|$, and λ is a nonnegative tuning parameter controlling the matrix sparsity, a larger λ value willl result in a sparse matrix. The interested reader can refer to [6] for the detailed graphical lasso algorithm.

In order to infer a signaling subnetwork of ER stress, we applied the graphical lasso algorithm (R package glassopath) to analyze the microarray data (Gene Expression Omnibus (GEO) access no. GSE19519) of immortalized B Cells [5] with 60 subjects which were treated by tunicamycin for 8 hours, a drug that can inhibit protein folding and modification in the ER, to induce ER stress. Undirected subnetworks of gene interactions, encoded by a sparse precision matrix, are inferred from twenty two genes which have been identified as important players in the ER stress signaling in the previous studies.

Figure 1 illustrates two inferred signaling subnetworks in response to ER stress with different values of tuning parameter λ. Though graphical lasso is very popular and it has been widely modified and applied to reconstruct gene regulatory network, our results in Fig. 1 demonstrates that, this algorithm is very sensitive to the values of tuning parameter λ. Most of the inferred edges are not consistent with some well-known models due to the noise in the microarray data. Moreover, graphical lasso can only infer undirected networks, however, the activation or inhibition information is also important to help us investigate the mechanism underlying the ER stress. Next we will build a directed ER stress-induced signaling pathway model based on literature searching and some well-known models.

3 Crosstalk of Stress-induced Signaling Pathways

Crosstalk of ER stress-induced signaling pathways, including ATF6, PERK and IRE1 pathways, have been summarized in our recent work [14, 15]. In this work, we will briefly reiterate some important pathways that are regulated by the ER membrane-associated transmembrane proteins. The crosstalk of these signaling components is depicted in the Figure 2 which was modified from [14, 15], where each node represents a regulatory component (protein or mRNA), the solid lines with arrows represent either protein transcription or changes of molecular species, dashed lines with arrows represent activation processes. We use a subscript "a/p" to describe an active or phosphorylated form of protein, while, the one without subscript represents an inactive molecule. Our objective is to develop a stochastic simulation model and apply probabilistic verification method to investigate the dynamic and temporal behaviors of these pathways during the pathogenesis of cancer and Alzheimer's disease, and predict the cell's fate in response to ER stress.

ATF6 pathway is activated with the help of coat protein II (COPII) complex in response to ER stress, ER transmembrane protein ATF6 is transported to the Golgi apparatus [22] where it is processed/cleaved by the site 1 protease (S1P) and S2P (S1/2P in Fig. 2), releasing the N-terminal cytosolic domain fragment ATF6f, an active form of ATF6. Upon activation, ATF6f enters the nucleus to activate the ER stress response element-dependent gene product X-box-binding protein 1 (XBP1) [22, 32], and upregulate the synthesis of cMYC and Cyclin D which will drive G1/S phase transition in the cell cycle.

In response to ER stress or abnormal accumulation of misfolded proteins, PERK can phosphorylate and activate the α-subunit of eIF2 (eukaryotic translation initiation factor-2), leading to the activation of P53-dependent apoptosis signaling pathway [39] through regulating the downstream tumor suppressor genes including ATF4 (activating transcription factor-4), CHOP and GADD34. PERK pathway's activation can reduce protein synthesis and stress in ER. In the normal cell, MDM2's phosphorylation is regulated by the oncoprotein

AKT and inhibited by PTEN, and the tumor suppressor P53's transcription activity is inhibited by the phosphorylated MDM2 in the nucleus which can promote the degradation of P53. P53 is also a transcription factor for MDM2, forming a negative feedback loop between P53 and MDM2. In this pathway, P53 and eIF2 are frequently mutated or down-regulated in the cells of cancer and neurodegenerative diseases [4].

IRE1 pathway plays an important role in the cell's inflammation, apoptosis, survival and Amyloid-β production [22, 32] induced by the ER stress. The interaction between IRE1 and TRAF2 (tumor necrosis factor receptor associated factor-2) will activate NFκB and JNK pathways. JNK pathway, which is activated by ASK1 (Apoptosis signal-regulating kinase 1), can regulate the synthesis of BACE1 (beta-secretase) and production of Amyloid-β (Aβ) [22, 21], whose abnormal accumulation is one of the major hallmarks in Alzheimer's disease. NFκB pathway regulates the transcription of several genes which play an important role in the cell growth, imflammation, and apoptosis: $TRAF2 \rightarrow IKK \dashv I\kappa B \dashv NF\kappa B$. In the resting cell, the tumor suppressor protein IκB binds to NFκB and forms a complex in the cytoplasm to inhibit its transcription activity. Some oncoproteins could activate IKK (IκB kinase), leading to the disassembly of IκB-NFκB complex (I-NFkB in Fig. 2). After NFκB translocates into the nucleus, it will promote the transcription of Cyclin D, BACE1, IκB and A20 [34, 20].

4 Probabilistic Verification Method

4.1 Time-bounded Linear Temporal Logic

Model checking [3] is a formal verification technique which can automatically determine whether or not some desired property is satisfied by a proposed model. A finite-state concurrent system is represented by a Kripke structrue [13, 3] $M = (S, s_0, R, L)$ in formal studies, where $s_0 \in S$ is an initial state, R is a transition relation between states S, and L is a function that labels each state S with the set of atomic propositions (AP) true in that state. The desired property is represented as a temporal logic formula ϕ, then, the model checking problem is expressed as: $M, s_0 \models \phi$.

Given a stochastic model M with a starting state s_0, a temporal logic formula ϕ, and a threshold value $\theta \in [0, 1]$ describing a pre-defined probability, then, the probabilistic model checking (PMC) problem is to decide whether $M, s_0 \models Pr_{\geq\theta}[\phi]$ is true or not. That is, the property ϕ is satisfied by M with a probability greater or equal to θ. Probabilistic model checker can also estimate the probability $Pr[\phi]$ such that ϕ satisfies M. Linear temporal logic (LTL) formulas, which describe properties of an "infinite" sequence of states, will be used to abstract the phenomenon in the biological system. The semantics of time-bounded LTL is defined with respect to the simulation trace of a stochastic system. We use σ^k to denote the trace starting at the step k, then, $\sigma^k \models \phi$ represents the trace σ^k satisfying the bounded LTL formula ϕ.

LTL formula is constructed from a set of APs, Boolean logic connectives, and *temporal* operators **X, F, G, U** describing the properties of a path [13, 3]. In the stochastic model M, we will use time-bounded temporal logic formulas to specify some desired properties. Time-bounded **F**, **G**, and **U** operators are defined as: $\mathbf{F}^t\phi$ or $\mathbf{F}(\leq t)[\phi]$ means ϕ holds true within time t; $\mathbf{G}^t\phi$ or $\mathbf{G}(\leq t)[\phi]$ means ϕ holds true globally up to time t; the time-bounded until operator $\phi_1\mathbf{U}^t\phi_2$ or $\phi_1\mathbf{U}(\leq t)\phi_2$ means, *within* time t, ϕ_1 will hold until ϕ_2 becomes true. We can also build composite operators using these basic LTL operators, for example,

$F^{t_1}G^{t_2}[\phi]$ or $F(\leq t_1)G(\leq t_2)[\phi]$ means, ϕ holds true within time t_1 and will be globally true up to time t_2. The syntax of the LTL logic is expressed as $\phi ::= AP \mid \phi_1 \vee \phi_2 \mid \phi_1 \wedge \phi_2 \mid \neg\phi_1 \mid \phi_1 \mathbf{U}^t \phi_2$. The interested readers could refer to [14, 15] for the detailed semantics of time-bounded LTL.

4.2 PRISM Model Checker

PRISM is an open-source probabilistic model checker, which has been widely used for the modeling and verification of different probabilistic systems [23, 24]. Besides simulation, PRISM supports the verification of different types of probabilistic models, including the discrete-time Markov chains, Markov decision processes, continuous-time Markov chains (CTMCs) models, and extensions of these models with rewards. Fig. 3 gives an example to illustrate the procedure to develop a PRISM model and apply it to analyze the ER stress-induced signaling pathways. Since the proposed model is a continuous-time stochastic process, the PRISM model file is given an extension ".sm", and the PRISM code starts with the keyword **ctmc**.

A PRISM program can consist of several modules which represent different components being modelled using the keywords "**module ... endmodule**". In this work, there is only one module "module ER" which describes the interactions of different proteins in the network. The state of the module is described by a set of variables, which take finite values (integer, Boolean) at different time points. The variables should be declared and initialized with the keyword **init** first. For example, "AKTp: [0..**N**] **init** 0;" means, the state or expression level of AKTp takes a finite number of integer values ranging from 0 to N, and its initial value is specified (as 0); the statement "Apoptosis: **bool init** false; " means, "Apoptosis" is a Boolean variable with an initial value false. In the PRISM code, the values of some constants, for example the constants of reaction rate, (de)activation and (de)phosphorylation rate, are defined with the keyword **const**.

The behavior of the module, that is the state changes, is specified by the "guard" and "updates" commands taking the form:

$$[action]\ guard \rightarrow rates : updates,$$

where *action* is a label (optional), *guard* is predicate of the model. PRISM supports both synchronous and asynchronous update of modules. Each guarded command with an empty square bracket [] corresponds to an asynchronous process. Some transitions having the same label placed in the square brackets in different modules will be updated simultaneously. The signal transduction in this work is a stochastic process and each reaction occurs at different rates, so, the state update of each variable is asynchronous. If the $guard$ is true, the states in the module will be updated according to "$updates$" with a rate of "$rates$" (≥ 0). The $updates$ can have more than one statement in the form of $V' = f(V)$, indicating that the variable V's value is updated to V'. That is,

$$V_1' = f(V_1)\ \&\ V_2' = f(V_2)\ \&\ ...\ \&\ V_k' = f(V_k),$$

where $V_1, V_2, ..., V_k$ are variables in the module.

4.3 Property Specification

Some properties based on temporal logic will be specified for PRISM model checker to automatically and formally verify the continuous-time Markov chain models. The continous

stochastic logic (CSL), which is a property specification language for CTMC process, is frequently used to specify the temporal properties in PRISM. The operator "**P**" refers to the probability that a given model satisfies some property. PRISM can formally analyze the following two types of properties:

1. $\mathbf{P}_{\geq p}\ [\phi]$ or $P_{\leq p}\ [\phi]$: is it true or false such that, the probability that ϕ satisfies the model M is at least or at most p (a pre-defined value)?

2. $\mathbf{P}_{=?}[\phi]$: what is the probability that ϕ satisfies the model M?

The first type of property is an assertion, the output will be either "True" or "False". PRISM can generate a succession of simulation traces to verify a time-bounded temporal logic formula on-the-fly based on the Wald's sequential probability ratio test (SPRT). SPRT is dependent on two parameters: δ denotes the half-width of an indifference region $[p - \delta, p + \delta]$, and "α/β" represents the probability of type I/II error. When an answer ("True", "False") can be given with a high confidence, PRISM will stop generating new traces, which is similar to the statistical model checking based on hypothesis testing [12]. Fig. 4 illustrates some temporal logic formulas which describe the properties in the ER stress-induced signaling pathway model. For example, the property "$P_{>=p}\ [\mathbf{F}_{<=t}\ (CyclinD \geq 500)]$" means, within t minutes, the number of CyclinD molecules in the cell will be at least 500 with a probability greater than or equal to $p(= 0.9)$.

PRISM could also directly evaluate a numerical value of a bounded property $P_{=?}[\phi]$ using confidence interval (CI) estimation method, which is dependent on two parameters, α (confidence coefficient) and ω (half-width of the interval), or N (number of samples). For example, "$P_{=?}\ [\mathbf{G}_{[80,100]}\ NFkBp/NFkBt \leq 0.35]$" estimates the probability that at most 35% of NFκB molecules always stay in the nucleus during the time interval [80, 100]. Given two temporal logic formulas ϕ_1 and ϕ_2, we can also estimate the conditional probability $P_{=?}(\phi_1|\phi_2) = P_{=?}(\phi_1 \& \phi_2)/P_{=?}(\phi_2)$ if $P_{=?}(\phi_2) \neq 0$.

5 Results

5.1 Stochastic Simulation

In this section, we will apply PRISM to analyze the ER stress-induced signaling pathways and investigate how the perturbation of these pathways influence the pathogenesis of cancer and neurodegenerative disease. In this model, we assume some regulatory components can take two possible forms, either active (phosphorylated) or inactive (unphosphorylated). All proteins are expressed in the number of molecules; and the subscript "t/i" represents the total/initial number of molecules. We assume the total number of molecules for some substrates (active + inactive) is constant. For example, AKT + AKT_p = $\text{AKT}_t = 10^4$. The values of most parameters are either abstracted from our previous work [12, 11] and other literatures or estimated from the experiments. The full PRISM code with parameters is available on http://cs.slu.edu/∼gong/research/IJDMB.zip.

Figure 5 demonstrates some stochastic simulation results of the proteins P53, MDM2, NFκB, IκB-NFκB, Cyclin D and Aβ's expression level changes over time. Fig. 5 (A-B) shows that, ER stress (a large number of ATF6, IRE1, PERK molecules) will promote P53's expression in the beginning, leading to the apoptosis. However, long-term stress will inhibit P53's expression and upregulate MDM2, CyclinD and Aβ's expression level, which will

induce uncontrolled cell cycle progression and abnormal accumulation of Amyloid-β, a hallmark of Alzheimer's disease. Fig. 5(C) shows the temporal behavior of NFκB and IκB-NFκB complex. Under the ER stress, IKK will be activated by the TRAF2, leading to the disassembly of IκB-NFκB complex. Free NFκB will then translocate into the nucleus to activate the transcription of several genes, including its inhibitors A20 and IκB, which can inhibit NFκB's activity, leading to negative feedback loops. The oscillation phenomenon in Fig. 5 (C) is consistent with the wet lab experiment [20, 29].

5.2 Formal Verification - SPRT

Next, we will apply the probabilistic model checking technique to verify or falsify some important temporal properties. We will first verify whether or not the probability that a model satisfies some given time-bounded LTL formulas is at least p. We set $\delta = \alpha = \beta = 0.05$ in the SPRT. Four different hypotheses are proposed and tested.

Hypothesis I: ER stress will promote the expression of oncoprotein Cyclin D and AD-associated protein Amyloid-β. The following three temporal logic formulas were checked:

$\mathbf{P}_{\geq 0.9}(\phi_1) = \mathbf{P}_{\geq 0.9}\ [F_{\leq t}\ (CyclinD \geq 500)]$;
$\mathbf{P}_{\geq 0.9}(\phi_1') = \mathbf{P}_{\geq 0.9}\ [F_{\leq t}\ (A\beta \geq 300)]$;
$\mathbf{P}_{\geq 0.9}(\phi_1'') = \mathbf{P}_{\geq 0.9}\ [F_{\leq 100}\ (Survival = true)]$.

A single simulation trace in Fig. 5(B) has verified this hypothesis, is this property always true? Formulas ϕ_1 and ϕ_1' mean that, if PERK, IRE1 and ATF6 are overexpressed (with an initial value 10^3), within t minutes, the number of Cyclin D and Amyloid-β molecules will be equal to or greater than a threshold value, these formulas are true with a probability of at least 0.9. These formulas were checked to be true with $t > 50$ minutes around, which confirmed our recent work [14] using symbolic model checker that overexpressed ER transmembrane proteins will finally promote the transcription of Amyloid-β peptides and Cyclin D, inducing cell to reach a state of "Alzheimer = True" and "Cancer=True" on all paths. PRISM also verified a Boolean property ϕ_1'': the cell will make transition from G1 to S phase when the number of Cyclin D molecules is above a threshold value within 100 minutes, which explained why long time ER stress could induce the pathogenesis of cancer and Alzheimer's disease [28, 25].

Hypothesis II: ER stress can induce apoptosis in the early stage through activating the P53 signaling pathway; however, the tumor suppressor P53's expression is inhibited, and oncoprotein MDM2's level is upregulated in the long term. Four formulas below were checked:

$\mathbf{P}_{\geq 0.9}(\phi_2) = \mathbf{P}_{\geq 0.9}\ \{F_{\leq t}\ (P53/P53i \geq a)\}$;
$\mathbf{P}_{\geq 0.9}(\phi_2') = \mathbf{P}_{\geq 0.9}\ \{G_{[20,t_1]}\ (P53/P53i \geq a)\}$;
$\mathbf{P}_{\geq 0.9}(\phi_2'') = \mathbf{P}_{\geq 0.9}\ \{F_{\leq t_2}\ (\frac{P53}{P53i} \leq b\ \&\ \frac{MDM2p}{MDM2i} \geq a)\}$;
$\mathbf{P}_{\geq 0.9}(\phi_2''') = \mathbf{P}_{\geq 0.9}\ [F_{\leq 50}\ (Apoptosis = true)]$.

Formula ϕ_2 means, within t (around 20) minutes, P53's expression level will be increased to be at least $a = 10$ times of its initial value, and it is verified to be true by PRISM. Formula ϕ_2' ($P53i$ denotes the initial value of $P53$) was also true when $t_1 = 25$,

that is, the number of P53 molecules continuously stays at a high level in a short time interval $[20, 25]$, but falsified if t_1 is given a large value. The verification of ϕ_2 and ϕ_2' is consistent with our previous SMV results [14] which state that ER stress could promote both apoptosis- and survival-related signal transductions. The verified formula ϕ_2'' claims, prolonged ER stress (within $t_2 = 80$ minutes) will promote the oncoprotein MDM2's phosphorylation ($a = 10$) which can inhibit P53's transcription activity ($b = 1$). Similar to Hypothesis I, we also verified a Boolean property ϕ_2''': Apoptosis is activated immediately after P53's expression level increases to ten times of its initial value due to the ER stress. These results are also consistent with the one single simulation trace in the Fig. 5(A).

Hypothesis III: In response to the external stimulus or stress, a large amount of NFκB will be disassembled from the IκB-NFκB complex and translocate into the nucleus to promote the transcription of many oncogenes and tumor suppressors. Three properties related to the ratio of free NFκB with the total number of NFκB molecules ($NF\kappa Bt$) in different time intervals were checked.

$\mathbf{P}_{\geq 0.9}(\phi_3) = \mathbf{P}_{\geq 0.9}\ [F_{\leq 30}(NF\kappa Bp/NF\kappa Bt \geq 0.5)]$;
$\mathbf{P}_{\geq 0.9}(\phi_3') = \mathbf{P}_{\geq 0.9}\ [F_{[60,80]}(NF\kappa Bp/NF\kappa Bt \leq 0.35)]$;
$\mathbf{P}_{\geq 0.9}(\phi_3'') = \mathbf{P}_{\geq 0.9}\ [G_{[80,100]}(NF\kappa Bp/NF\kappa Bt \leq 0.35)]$.

Formulas $\phi_3 - \phi_3'$ predict, half of NFκB molecules will be disassembled from the IκB-NFκB complex and translocate into the nucleus within 30 minutes after ER stress, then, during the time interval $[60, 80]$, the percentage of nuclear NFκB will be reduced to a threshold value due to a negative feedback loop regulated by IκB and A20. These two formulas were verified to be true by PRISM. However, the formula ϕ_3'' is falsified, that is, in the long run ([80, 100]), NFκB's expression level in the nucleus is fluctuating or oscillating instead of (globally) stable which has been observed in the wet lab experiment [20].

Hypothesis IV: Overexpressed IKK can increase the number of free NFκB molecules and promote its translocation into the nucleus to induce the transcription of Cyclin D which regulates the G1/S phase transition. That is, changing the expression level of IKK will influence the levels of CyclinD, Aβ and NFκB.

Table 1: Verification of Hypothesis IV

IKK($\times 10^3$)	1.0	2.5	5.0	7.5	10	15	20
$\mathbf{P}_{\geq 0.9}(\phi_1), t = 50$	False	False	False	False	True	True	True
$\mathbf{P}_{\geq 0.9}(\phi_1'), t = 50$	False	True	True	True	True	True	True
$\mathbf{P}_{\geq 0.9}(\phi_3)$	False	False	False	True	True	True	True
$\mathbf{P}_{\geq 0.9}(\phi_3')$	True	True	True	True	True	False	False
$\mathbf{P}_{\geq 0.9}(\phi_3'')$	True	True	True	False	False	False	False

IKK is an oncoprotein which can inhibit NFκB's transcription activity. We vary IKK's initial value to investigate how it influences the expression level of Cyclin D and NFκB, that is, checking the formulas in Hypothesis I and III. The verification results in Table 1 confirmed that overexpressed IKK could eventually promote the transcription of Cyclin D and increase the number of free NFκB molecules in the nucleus, which plays an important role in the tumorigenesis, inflammation and Alzheimer's disease; while a smaller initial value of IKK could reduce the amount of NFκB molecules in the nucleus. These results

are consistent with previous studies [10, 11, 13, 14]. The verification of hypothesis IV explained why inhibiting the NFκB pathway with IKK inhibitor (e.g., Manumycin A) could repress tumorigenesis, and this pathway is also a potential therapeutic target for Alzheimer's disease.

The time-bounded temporal logic formulas in the Hypothesis I-IV are assertions of temporal properties in the pathway model. Given a predefined probability $p = 0.9$, the PRISM model checker will output either "True" or "False" based on a Wald's sequential probability ratio test. In many cases, we need directly estimate the probability that a temporal logic property is satisfied by a model. Below, we perform a more accurate estimation of some temporal properties using PRISM based on the confidence interval estimation method.

5.3 Formal Verification - Estimation

Estimation I: Find the probability that the number of Cyclin D and Aβ molecules will be equal to or greater than a threshold value, and the cell will reach S phase (Survival) within time t?

$\mathbf{P}_{=?}(\phi_1) = \mathbf{P}_{=?}\ [F_{\leq t}(CyclinD \geq 500)]$;
$\mathbf{P}_{=?}(\phi_1') = \mathbf{P}_{=?}\ [F_{\leq t}(A\beta \geq 300)]$;
$\mathbf{P}_{=?}(\phi_1'') = \mathbf{P}_{=?}\ [F_{\leq t}\ (Survival = true)]$.

Table 2: Results of Estimation I							
time (t)	30	35	40	45	50	60	70
$\mathbf{P}_{=?}(\phi_1)$	1E-4	0.019	0.31	0.75	0.93	0.99	0.99
$\mathbf{P}_{=?}(\phi_1')$	0.122	0.984	1.0	1.0	1.0	1.0	1.0
$\mathbf{P}_{=?}(\phi_1'')$	0.0	0.007	0.29	0.69	0.91	0.99	0.99

We fix $\alpha = \omega$ = 0.05, and vary the time t to estimate the probabilities that $\phi_1 - \phi_1''$ are true, the verification results are listed in Table 2. These probabilities are increasing with time, which indicate that, prolonged ER stress (after around 1 hour) will definitely induce the uncontrolled cell cycle progression, abnormal synthesis and accumulation of Cyclin D and Amyloid-β molecules.

Estimation II: Estimate the probabilities of ϕ_2 and ϕ_2'' are true in Hypothesis II which describe the activity of P53's transcription and MDM2's phosphorylation in response to ER stress.

$\mathbf{P}_{=?}(\phi_2) = \mathbf{P}_{=?}\ \{F_{\leq 20}\ (P53/P53i \geq a)\}$;
$\mathbf{P}_{=?}(\phi_2') = \mathbf{P}_{=?}\ \{G_{[20,25]}\ (P53/P53i \geq a)\}$;
$\mathbf{P}_{=?}(\phi_2'') = \mathbf{P}_{=?}\ \{F_{\leq 80}\ (\frac{P53}{P53i} \leq b\ \&\ \frac{MDM2p}{MDM2i} \geq c)\}$.

Table 3: Results of Estimation II							
a	8	9	10	11	12	13	14
$\mathbf{P}_{=?}(\phi_2)$	1.00	1.00	0.996	0.97	0.60	0.02	0.0
$\mathbf{P}_{=?}(\phi_2')$	1.00	0.99	0.93	0.74	0.45	0.02	0.0
$b\ (c = 10)$	0.25	0.50	0.75	1.0	1.5	2.0	2.5
$\mathbf{P}_{=?}(\phi_2'')$	1E-4	0.02	0.6	0.92	0.92	0.93	0.93

Table 3 reports the results with different values of a and/or b ($\alpha = \omega = 0.05$). The estimated probabilities are consistent with the SPRT results, that is, P53's expression level will be upregulated (increase at least 11 times of the initial value) immediately after external stress. However, it will reduce to a lower level (around its initial value) in the long term due to the negative regulation by MDM2 which is upregulated by the ER stress pathways within 80 minutes.

Estimation III: What is the percentage of free NFκB molecules in the nucleus after ER stress, and estimate the probabilities that the formulas in the hypothesis III hold under different conditions.

$\mathbf{P}_{=?}(\phi_3) = \mathbf{P}_{=?}\ [F_{\leq 30}(NF\kappa Bp/NF\kappa Bt \geq a)]$;
$\mathbf{P}_{=?}(\phi_3') = \mathbf{P}_{=?}\ [F_{[60,T]}(NF\kappa Bp/NF\kappa Bt \leq 0.35)]$.

Table 4: Results of Estimation III							
a	0.50	0.52	0.55	0.56	0.58	0.60	0.62
$\mathbf{P}_{=?}(\phi_3)$	1.0	1.0	0.85	0.52	0.04	0.01	0.00
T	63	65	67	70	75	80	85
$\mathbf{P}_{=?}(\phi_3')$	0.38	0.61	0.82	0.95	1.0	1.0	1.0

During verification, we fix α = 0.05, N = 100 and vary the values of different parameters. Table 4 reports the estimated probabilities of some formulas in the hypothesis III and IV. The first two rows' results show that, the percentage of NFκB in the nucleus hits the peak (a's value is around 0.5$\sim$0.55) within 30 minutes after stress. We can also determine when this percentage will reduce to a given value through varying T's value, which indicates that, after around 70 minutes, most of NFκB are taken out of the nucleus by its inhibitor IκB and inhibited by A20 due to the negative feedback loops.

Estimation IV: Varying the IKK's initial values under different conditions, estimate the probabilities that the two formulas in the Hypothesis III together with the property ϕ_3'' hold:

$\mathbf{P}_{=?}(\phi_3'') = \mathbf{P}_{=?}\ [G_{[80,100]}(NF\kappa Bp/NF\kappa Bt \leq 0.35)]$.

Table 5: Results of Estimation IV							
IKK ($\times 10^3$)	5.0	6.0	7.5	9.0	10	15	20
$\mathbf{P}_{=?}(\phi_3)$, $a = 0.5$	0.45	0.99	1.0	1.0	1.0	1.0	1.0
$\mathbf{P}_{=?}(\phi_3')$, $T = 80$	1.0	1.0	1.0	1.0	1.0	0.88	0.41
$\mathbf{P}_{=?}(\phi_3'')$	0.99	0.89	0.25	1E-4	0.0	0.0	0.0

Table 5 lists the probabilities of these properties hold in Hypothesis IV with different initial values of IKK. These results confirmed that, overexpressed IKK will increase the percentage of free NFκB in the nucleus, that is, $\mathbf{P}_{=?}(\phi_3) = 1$. However, we will observe a large probability that the percentage of NFκB molecules in the nucleus will be reduced with a smaller initial value of IKK, that is $\mathbf{P}_{=?}(\phi_3') \rightarrow 1$ and $\mathbf{P}_{=?}(\phi_3'') \rightarrow 1$. These results are consistent with the qualitative assertations in Table 1.

Estimation V: Given $\phi_4 = F_{\leq 80}\ (\frac{MDM2p}{MDM2i} \geq 10\ )$, and $\phi_5 = F_{\leq 80}\ (\frac{P53}{P53i} \leq a\ )$, estimate the conditional probability $\mathbf{P}_{=?}(\phi_5|\phi_4) = \frac{P_{=?}\ \{F_{\leq 80}\ (\frac{P53}{P53i} \leq a\ \&\ \frac{MDM2p}{MDM2i} \geq 10)\}}{P_{=?}\ \{F_{\leq 80}\ (\frac{MDM2p}{MDM2i} \geq 10)\}}$.

Table 6: Conditional Probability Estimation							
a	0.25	0.50	0.75	1.00	1.50	2.00	2.50
$\mathbf{P}_{=?}(\phi_5\|\phi_4)$	0.00	0.02	0.63	0.96	0.96	0.97	0.97

Table 6 lists the estimated conditional probabilities through varying the value of a (with fixed $\alpha = \omega = 0.05$), which is the ratio of P53 and its initial value. Using PRISM, we can first estimate $\mathbf{P}_{=?}(\phi_4)$ = $\mathbf{P}_{=?}(F_{\leq 80}\ (\frac{MDM2p}{MDM2i} \geq 10)) = 0.957$. The estimated conditional probability values indicate that, given a large number of phosphorylated MDM2 molecules, P53's expression level will be reduced below its initial value with a high probability.

6 Conclusion

ER stress-induced signaling pathways are implicated in the pathogenesis of several diseases, and it is still not clear that how do they influence the cell's fate. In this work, we first applied a graphical lasso method to infer undirected models of signaling subnetwork induced by ER stress. Due to the noise of microarray data, these models are very sensitive to the tuning parameters. Then, we developed a stochastic model based on literature searching to describe the crosstalk of different signaling pathways. Finally, a probabilistic model checker, PRISM which is based on sequential probability ratio test and confidence interval estimation methods, is applied to formally analyze some important quantitative properties of the system expressed as temporal logic formulas, some of which are difficult to be addressed using the traditional simulation approaches. Our recent work [14] applied symbolic model verification (SMV) technique to formally analyze both asynchronous and synchronous discrete-value models of ER-Golgi network. Compared with the SMV study, this work could not only qualitatively analyze the complex biological system, but also provide a "quantitative" estimation of some properties. However, we remark that, since many reaction rate constants and parameters in our model are unknown or indirectly estimated or tuned from existing experiments, the current model can only qualitatively compare with the experimental behavior.

Probabilistic verification of the temporal logic formulas using hypothesis testing and estimation methods shows that, overexpressed ER transmembrane sensor proteins will promote the expression of Cyclin D, Amyloid-β and MDM2, leading to the pathogenesis of cancer and AD in the long term, and inhibit apoptosis. ER stress could also promote the translocation of NFκB to the nucleus, whose expression level is fluctuating due to the negative feedback loops composed of IKK, IκB, NFκB and A20, which has been observed in Hoffmann et al's experiment [20]. Our work continues to verify that, varying IKK's initial value will influence the number of Aβ and free NFκB molecules in the nucleus. These results provide valuable insights into the ER stress mechanism, and explain why NFκB could be a potential therapeutic target for the tumorigenesis and Alzheimer's disease.

The proposed crosstalk model of signaling pathways is composed of three signaling branches initiated by ER-resident transmembrane proteins in response to ER stress, and the model construction is based on literature searching only. However, ER and its neighboring compartment Golgi apparatus regulate many signaling and secretory pathways which are

of importance in the cell cycle progression. In order to comprehensively investigate the roles of ER stress in the pathogenesis of cancer and other diseases, a larger network which incorporates all the important regulatory components is necessary. With more publicly available gene expression data, our future work will integrate the statistical inference algorithms with the model checking technique together to reconstruct and verify the ER stress-induced signaling pathways.

Authors' contributions

H.G. and Y.G proposed the project, Y.M wrote the graphical lasso code and analyze the microarray data, L.F. and H.G. wrote the PRISM code and performed the analysis.

Acknowledgment

This work was partially supported by H.G.'s new faculty start-up grant and President Research Fund award (230152) from the Saint Louis University.

References

[1] David G Breckenridge. Regulation of apoptosis by endoplasmic reticulum pathways. *Oncogene*, 22, 2003.

[2] E. M. Clarke, J. R. Faeder, L. A. Harris, C. J. Langmead, A. Legay, and S. K. Jha. Statistical model checking in biolab: Applications to the automated analysis of t-cell receptor signaling pathway. 5307:231–250, 2008.

[3] E. M. Clarke, O. Grumberg, and D. A. Peled. *Model Checking*. MIT Press, 1999.

[4] MartÃn de la Vega C et al. Possible mechanisms involved in the down-regulation of translation during transient global ischaemia in the rat brain. *Biochem J.*, 357, 2001.

[5] Beth Dombroski, Renuka Nayak, et al. Gene expression and genetic variation in response to endoplasmic reticulum stress in human cells. *The American Journal of Human Genetics*, 86:719–929, 2010.

[6] J Friedman, T. Hastie, and R Tibshirani. Sparse inverse covariance estimation with the graphical lasso. *Biostatistics*, pages 1–10, 2007.

[7] D. T. Gillespie. A general method for numerically simulating the stochastic time evolution of coupled chemical reactions. *J. Comp. Phys.*, 22(4):403–434, 1976.

[8] H. Gong, Y. Guo, A. Linstedt, and R. Schwartz. Discrete, continuous, and stochastic models of protein sorting in the golgi apparatus. *Physical Review E*, 81(1):011914, 2010.

[9] H. Gong, H. Sengupta, A. Linstedt, and R. Schwartz. Simulated de novo assembly of golgi compartments by selective cargo capture during vesicle budding and targeted vesicle fusion. *Biophysical Journal*, 95:1674–1688, 2008.

[10] H. Gong, Q. Wang, P. Zuliani, M. T. Lotze, J. R. Faeder, and E. M. Clarke. Symbolic model checking of the signaling pathway in pancreatic cancer. *Proceedings of the International Conference on Bioinformatics and Computational Biology (BICoB)*, 2011.

[11] H. Gong, P. Zuliani, A. Komuravelli, J. Faeder, and E. Clarke. Computational modeling and verification of signaling pathways in cancer. *Proceedings of Algebraic and Numeric Biology, LNCS*, 6479, 2012.

[12] H. Gong, P. Zuliani, A. Komuravelli, J. R. Faeder, and E. M. Clarke. Analysis and verification of the HMGB1 signaling pathway. *BMC Bioinformatics*, 11(7), 2010.

[13] Haijun Gong. Analysis of intercellular signal transduction in the tumor microenvironment. *BMC Systems Biology*, 7:S5, 2013.

[14] Haijun Gong and Lu Feng. Computational analysis of the roles of er-golgi network in the cell cycle. *BMC Systems Biology*, 8:S4, 2014.

[15] Haijun Gong and Lu Feng. Probabilistic verification of er stress-induced signaling pathways. *Proceedings of IEEE International Conference on Bioinformatics and Biomedicine*, 2014.

[16] Haijun Gong, Jakob Klinger, Kevin Damazyn, Xiangrui Li, and Shiyang Huang. A novel procedure for statistical inference and verification of gene regulatory subnetwork. *BMC Bioinformatics*, V16:S7, 2015.

[17] Haijun Gong, Qinsi Wang, Paolo Zuliani, and Edmund Clarke. Formal analysis for logical models of pancreatic cancer. *50th IEEE Conference on Decision and Control and European Control Conference*, 2011.

[18] Haijun Gong, Tong Tong Wu, and Edmund M. Clarke. Pathway-gene identification for pancreatic cancer survival via doubly regularized cox regression. *BMC Systems Biology*, 8, 2014.

[19] Haijun Gong, Paolo Zuliani, and Edmund Clarke. Model checking of a diabetes-cancer model. *3rd International Symposium on Computational Models for Life Sciences*, 2011.

[20] A. Hoffmann, A. Levchenko, M.L. Scott, and D. Baltimore. The IκB-NFκB signaling module: Temporal control and selective gene activation. *Science*, 298:1241–1245, 2002.

[21] G Hotamisligil. Endoplasmic reticulum stress and the inflammatory basis of metabolic disease. *Cell*, 140, 2010.

[22] H Kadowaki and H Nishitoh. Signaling pathways from the endoplasmic reticulum and their roles in disease. *Genes*, 2013.

[23] M. Kwiatkowska, G. Norman, and J. Sproston. Probabilistic model checking of deadline properties in the ieee1394 firewire root contention protocol. *Formal Aspects of Computing*, 14:295–318, 2003.

[24] Marta Kwiatkowska, Gethin Norman, and David Parker. Probabilistic model checking in practice: Case studies with prism. *ACM SIGMETRICS Performance Evaluation Review*, 32:16–21, 2005.

[25] Bingqian Liu et al. Endoplasmic reticulum stress promotes amyloid-beta peptides production in rgc-5 cells. *Cell Stress and Chaperones*, 2014.

[26] Y. Luan and H. Li. Group additive regression models for genomic data analysis. *Biostatistics*, 9:100–113, 2008.

[27] S. Ma, X. Song, and J. Huang. Supervised group lasso with applications to microarray data analysis. *BMC Bioinformatics*, 8:60–76, 2007.

[28] Sara Mokhtar et al. The beta-amyloid protein of alzheimerâŁ™s disease: Communication breakdown by modifying the neuronal cytoskeleton. *International Journal of AlzheimerâŁ™s Disease*, 2013, 2013.

[29] D.E. Nelson, A.E.C. Ihekwaba, et al. Oscillations in NF-κB signaling control the dynamics of gene expression. *Science*, 306:704–708, 2004.

[30] Claudia Pereira. Crosstalk between endoplasmic reticulum stress and protein misfolding in neurodegenerative diseases. *ISRN Cell Biology*, 2013.

[31] D. Thomas Rutkowski and Randal J. Kaufman. A trip to the er: coping with stress. *Trends in Cell Biology*, 14, 2004.

[32] A Salminen et al. Er stress in alzheimer's disease: a novel neuronal trigger for inflammation and alzheimer's pathology. *Journal of Neuroinflammation*, 6, 2009.

[33] A. Statnikov, C. F. Aliferis, I. Tsamardinos, D. Hardin, and S. Levy. A comprehensive evaluation of multicategory classification methods for microarray gene expression cancer diagnosis. *Bioinformatics*, 21:631–643, 2005.

[34] J. R. van Beijnum, W. A. Buurman, and A. W. Griffioen. Convergence and amplification of toll-like receptor (tlr) and receptor for advanced glycation end products (rage) signaling pathways via high mobility group b1. *Angiogenesis*, 11:91–99, 2008.

[35] D Wlodkowic, J Skommer, et al. Er-golgi network - a future target for anti-cancer therapy. *Leuk Res*, 2009.

[36] T. T. Wu, Y. F. Chen, T. Hastie, E. Sobel, and K. Lange. Genomewide association analysis by lasso penalized logistic regression. *Bioinformatics*, 25:714–721, 2009.

[37] T. T. Wu and S. Wang. Doubly regularized cox regression for high-dimensional survival data with group structures. *Statisstics and Its Interface*, 6:175–186, 2013.

[38] Tong Tong Wu, Haijun Gong, and Edmund M. Clarke. A transcriptome analysis by lasso penalized cox regression for pancreatic cancer survival. *Journal of Bioinformatics and Computational Biology*, 9:63, 2011.

[39] A Yagi et al. Gadd34 induces p53 phosphorylation and p21/waf1 transcription. *J Cell Biochem*, 90(6):1242–9, 2003.

[40] M. Yuan and Y. Lin. Model selection and estimation in regression with grouped variables. *J. R. Statist. Soc. B*, 68:49–67, 2006.

[41] P. Zuliani, A. Platzer, and E. M. Clarke. Bayesian statistical model checking with application to simulink/stateflow verification. In *HSCC*, pages 243–252, 2010.

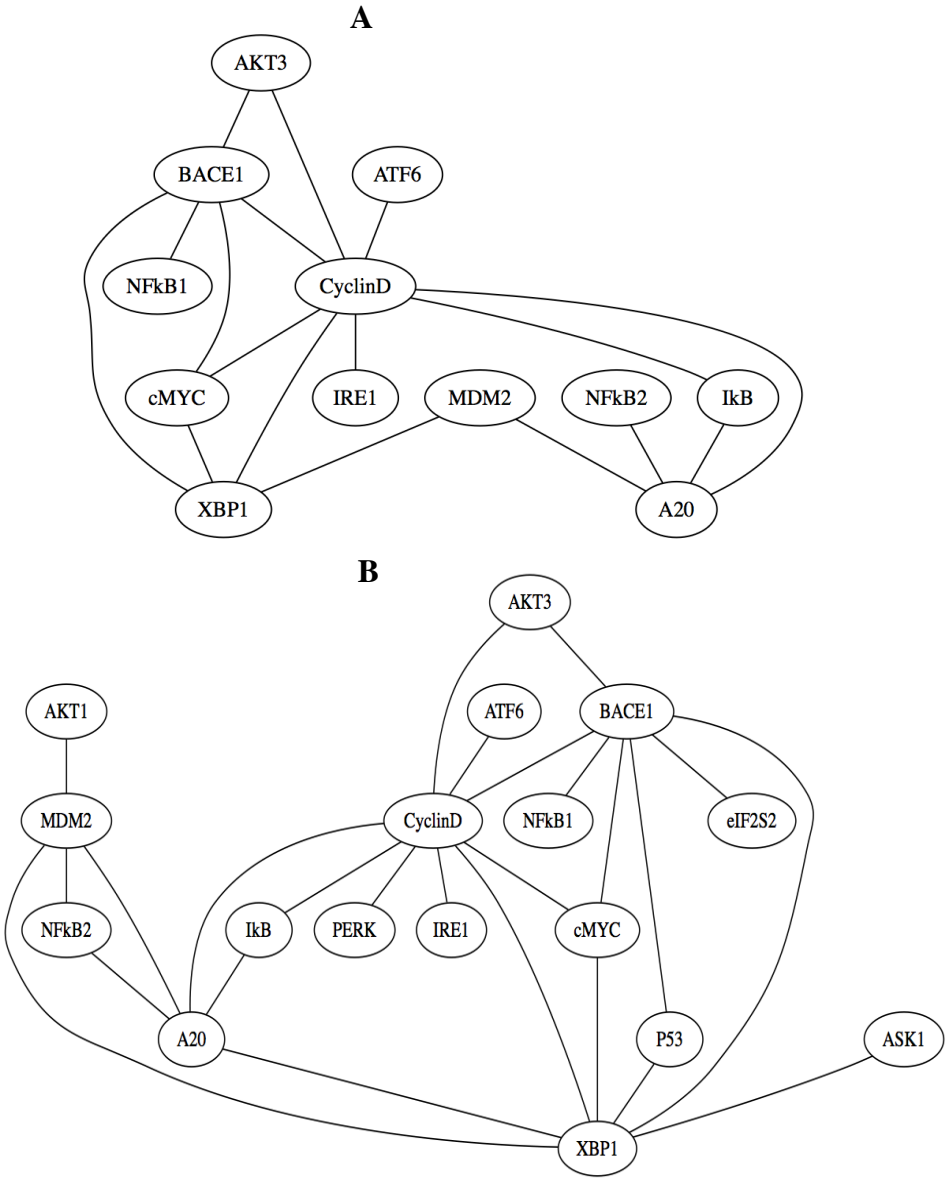

Figure 1 Inferred ER stress-induced signaling networks with different values of tuning parameter: (A) $\lambda = 0.1$, (B) $\lambda = 0.08$. Each node represents a gene, and each edge represents a conditional dependence.

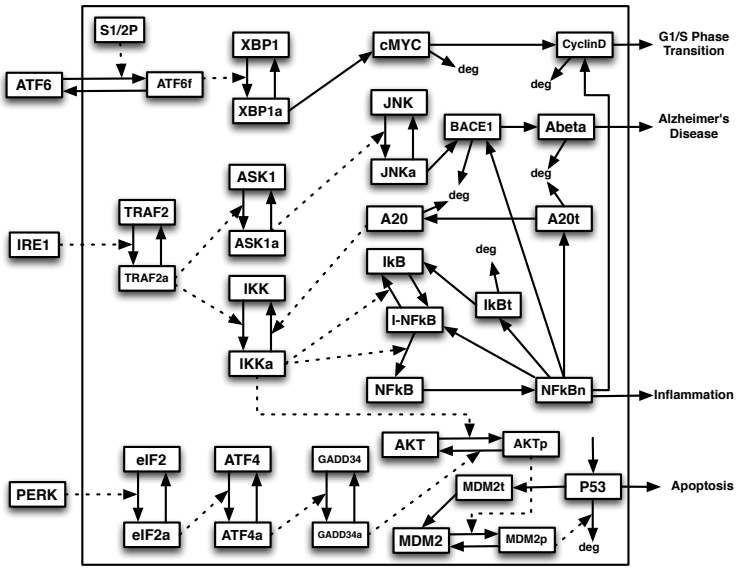

Figure 2 Crosstalk of ER stress-induced signaling pathways and four possible cell fates: each node represents a regulatory component; solid lines with arrows represent either protein transcription or changes of molecular species; dashed lines with arrows represent activation processes.

PRISM Model: ERprism.sm

```
  // Continuous time Markov chains (CTMC) model
ctmc
  // Declaration of constants
      const int N = 1000;
      const double k1 = 0.01;
      const double d1 = 0.01;
      ...
module ER
  // Variable declaration and initialization
      IKK: [0..N] init N;
      IKKa: [0..N] init 0;  // activated IKK
      AKT: [0..N] init N;  // unphosphorylated AKT
      AKTp: [0..N] init 0;  // phosphorylated AKT
      Apoptosis: bool init false;  // Apoptosis is Boolean Variable
      ...
  // State transition update
      // AKT is phosphorylated by IKKa
      [ ] IKKa>0 & AKT>0 → k1*IKKa*AKT: (AKTp'=AKTp + 1) & (AKT'=AKT - 1);

      //AKTp dephosphorylation
      [ ] AKTp>0 → d1*AKTp: (AKTp'=AKTp - 1) & (AKT'=AKT + 1);

      //Apoptosis occurs is P53 Level is High
      [ ] P53/NP53 ≥ 10 → 1: (Apoptosis' = true);
      ...
endmodule
```

Figure 3 An example of PRISM model for the simulation and verification of ER stress-induced signaling pathways

PRISM Property Specification: ERtest.csl

const double T;

$\mathbf{P}_{\geq 0.9}$ [$F <= T$ $(CyclinD >= 500)$];

$\mathbf{P}_{\geq 0.9}$ [$G[80,100]$ $(NFkBn/NFkBt <= 0.35)$];

$\mathbf{P}_{\geq 0.9}$ [$F_{\leq 50}$ $(Apoptosis = true)$];

$\mathbf{P}_{\geq 0.9}$ [$F <= T$ $(P53/P53i <= a$ & $(MDM2p/MDM2i >= b))$];

$\mathbf{P}_{=?}$ [$F <= T$ $(Abeta >= 300)$];

$\mathbf{P}_{=?}$ [$G[80,100]$ $(NFkBn/NFkBt <= 0.35)$];

$\mathbf{P}_{=?}$ [$F_{\leq 50}$ $(Apoptosis = true)$];

Figure 4 Illustration of property specifications for the PRISM model of ER stress-induced signaling pathway based on sequential probability ratio test and confidence interval estimation methods

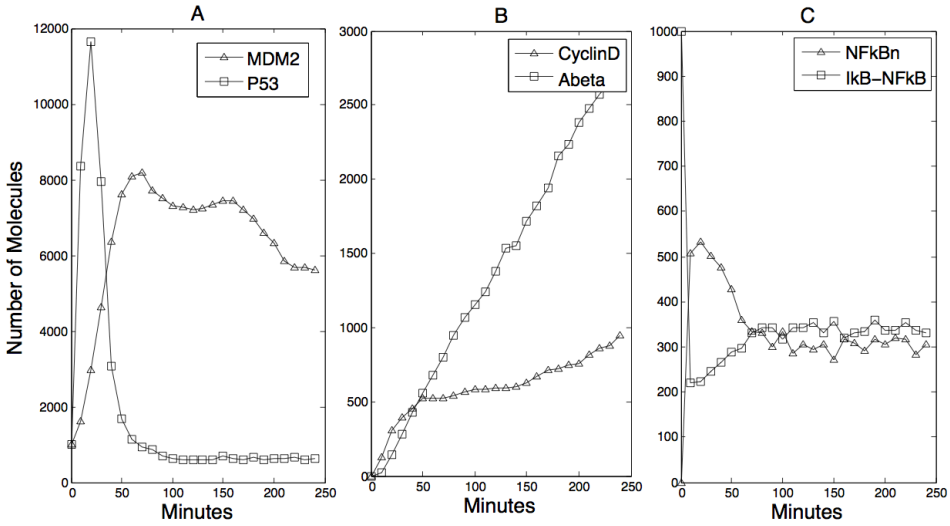

Figure 5 The time course of the expression level (number of molecules) of P53 and MDM2 (A); NFκB and IκB-NFκB (B); Cyclin D and Aβ (C) based on stochastic simulation method using PRISM.